Appl. Phys. B (2017) 123:80
DOI 10.1007/s00340-016-6631-5

Applied Physics B
Lasers and Optics

High-pulse-energy mid-infrared optical parametric oscillator based on $BaGa_4Se_7$ crystal pumped at 1.064 μm

Wen-Tao Xu[1,2] · Yu-ye Wang[1,2] · De-Gang Xu[1,2] · Chao Li[3] · Ji-Yong Yao[3] · Chao Yan[1,2] · Yi-Xin He[1,2] · Mei-tong Nie[1,2] · Yi-Cheng Wu[3] · Jian-quan Yao[1,2]

Received: 31 July 2016 / Accepted: 29 December 2016 / Published online: 4 March 2017

Abstract We have demonstrated a high-pulse-energy nanosecond mid-infrared optical parametric oscillator (OPO) based on the nonlinear crystal $BaGa_4Se_7$ pumped by 1.064 μm Nd:YAG laser. The experimental OPO threshold of 7.97 MW/cm^2 was in good agreement with the theoretical calculation of 8.05 MW/cm^2. The maximum pulse energy of the idler wavelength was 2.56 mJ at 4.11 μm wavelength when the pump energy was 61.6 mJ, corresponding to an optical-to-optical conversion efficiency of 4.16%. The idler wavelength can be continuously tuned in the range from 3.12 to 5.16 μm.

1 Introduction

High-pulse-energy laser sources tuning in the mid-infrared (MIR) range from 3 to 30 μm, are intensively required for a variety of applications in science and technology. Among the general methods, optical parametric oscillator (OPO) is an attractive approach which can generate high energy and widely tunable laser radiation simultaneously. With a conventional Nd-nanosecond laser systems emitting at ~1 μm, OPO has been proved to be an effective way to obtain coherent radiation in a broad MIR spectral wavelength range [1]. Nonlinear optical (NLO) crystals with wide transparent region, large NLO coefficient, and high laser damage threshold are desired for the parametric devices down-converting the laser frequency to the MIR region. Until now, there are some commercial oxide crystals can be used in the MIR region, such as KTP [2], KTA [3], and $LiNbO_3$ [4]. Such kind of the crystals are partially transparent in the MIR region but not more than 4–5 μm due to the onset of (two- or multi-) phonon absorption starting from about 4 μm. Therefore, the non-oxide crystals is necessary for the longer wavelength generation, such as arsenides, phosphides or chalcogenides (sulfides, selenides and tellurides). Many kinds of non-oxide crystals have been reported for the MIR range, but limited by the damage threshold, which is often lower than OPOs threshold. Up to now, several kind of crystals can be successfully used for generating MIR laser based on ~1 μm pumped OPOs [1], including Ag_3AsS_3 [5], $AgGaS_2$ [6], $HgGa_2S_4$ [7], $Cd_xHg_{1-x}Ga_2S_4$ [8], $LiInSe_2$ [9], $CdSiP_2$ [10], $LiGaS_2$ [11], $BaGa_4S_7$ [12] and OP-GaP [13] crystal. However, there is still an urgent need for new MIR NLO crystals.

The recently discovered selenide analogue $BaGa_4Se_7$ (BGSe) [14–16] crystal has been reported as a potential alternative NLO crystal for generating MIR radiation. The crystal is positive biaxial crystal and belongs to the m monoclinic point group, space group P_c, with $a = 7.6252(15)$ Å, $b = 6.5114(13)$ Å, $c = 14.702(4)$ Å, $\beta = 121.24(2)°$, and $Z = 2$. Single crystals of BGSe can be grown in a large size by the Bridgman–Stockbarger

✉ Yu-ye Wang
yuyewang@tju.edu.cn

✉ De-Gang Xu
xudegang@tju.edu.cn

✉ Ji-Yong Yao
jyao@mail.ipc.ac.cn

1 Institute of Laser and Optoelectronics, School of Precision Instrument and Optoelectronic Engineering, Tianjin University, Tianjin 300072, People's Republic of China

2 Key Laboratory of Optoelectronic Information Science and Technology (Ministry of Education), Tianjin University, Tianjin 300072, People's Republic of China

3 Beijing Center for Crystal R&D, Key Laboratory of Functional Crystal and Laser Technology, Technical Institute of Physics and Chemistry, Chinese Academy of Sciences, Beijing 100190, People's Republic of China

method and the SHG effect was confirmed by many researchers. It features relatively high NLO coefficients with the two major nonlinear tensor elements of $d_{11} = 24.3$ pm/V and $d_{13} = 20.4$ pm/V [17]. The correspondence between the dielectric (principal optical) axes *xyz* and the crystallographic axes *abc* in the monoclinic BGSe crystal, in which *c* coincides with the two-fold symmetry axis, is $xyz = bac$ if the convention $c_0 < a_0 < b_0$ is used for the lattice parameters. Furthermore, the angle Ω between the optical axes and the *z*-principal (dielectric) axis was measured to be $\Omega = 45.6°$ (under the convention $n_x < n_y < n_z$). Overall, the BGSe crystal shows a number of intriguing properties. For example, the transparent range of this crystal covers from 0.47 to 18 μm, which makes it possible to obtain MIR coherent light through parametric down-conversion. Moreover, the BGSe crystal has the characteristics of better thermos–mechanical properties, adequate birefringence to phase-matched (PM) and high laser damage threshold contributed by a relatively wide bandgap ($E_g = 2.64$ eV) [18]. Therefore, it can be deduced that the BGSe crystal is a very promising NLO crystal for practical applications in the MIR region.

Based on the BGSe crystal, a high efficiency and high peak power picosecond MIR optical parametric amplifier (OPA) was demonstrated in 2013. The peak power of ~27 MW and output energy of 830 μJ at 3.9 μm were achieved under a pump energy of ~9.1 mJ [19]. In 2015, a widely tunable picosecond BGSe OPA with wavelength ranging from 6.4 to 11 μm was achieved. Peak power of ~4.2 MW and output energy of ~125 μJ at 7.8 μm were obtained under a pump energy of ~9 mJ [20]. In 2016, a high power, tunable MIR $BaGa_4Se_7$ OPO pumped by a 2.1 μm Ho:YAG laser was demonstrated. The maximum output power of 1.55 W in the 3–5 μm range was realized under the pump power of 10.8 W [21]. Recently, a wide idler tunability of 2.7–17 μm based on $BaGa_4Se_7$ OPO has been reported. The maximum output energy of 3.7 mJ at ~7.2 μm with the pulse width about 10 ns was obtained under the 1064 nm pump energy of 63 mJ at 10 Hz. The pump-to-idler slope conversion efficiency at 7.2 μm was 6.5% [22].

In this paper, a single pump passing singly-resonant OPO (SSRO) based on the BGSe crystal pumped by a 1.064 μm Q-witched Nd:YAG laser was presented. The oscillator can be continuously tuned in the range from 3.12 to 5.16 μm. It provided 2.56 mJ pulse energy at 4.11 μm with 10 Hz repetition rate. The optical-to-optical conversion efficiency was 4.16% and the slope conversion efficiency at 1.8 μm was 7.7%. The peak power of signal wave amounted to about 256 kW.

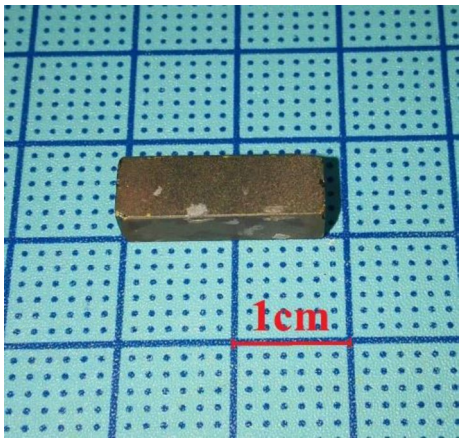

Fig. 1 Photograph of the BGSe crystal

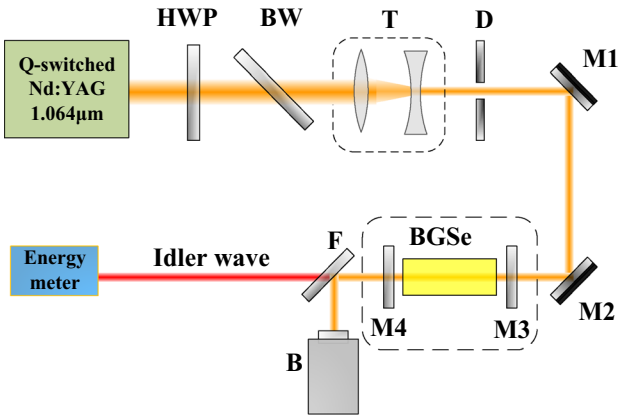

Fig. 2 Experimental setup of the 1.064 μm pumped BGSe–SSRO

2 Experimental setup

The BGSe crystal (5×5×17.3 mm) used in our MIR SSRO experiment, as shown in Fig. 1, was grown by the Bridgman-Stockbarger method. It is cut in the x–z plane at $\theta = 54.7°$ for ee-o type I phase-matching with the 5 mm edge parallel to the y axis, to ensure large effective nonlinearity d_{eff}. The effective nonlinear coefficient for this situation, is calculated by $d_{\text{eff}} = d_{16}\cos^2(\theta) + d_{23}\sin^2(\theta)$. Both the working faces of the crystal were polished and coated. The reflectance at each surface was less than 1% at 1.064 μm wavelength.

Figure 2 shows the experimental configurations of the 1.064 μm pumped BGSe–SSRO. The pump source was a diode-pumped electro-optical Q-switched Nd:YAG laser with a pulse repetition rate up to 100 Hz. The full width at half-maximum (FWHM) of the laser pulse was 16 ns as shown in Fig. 3, and the divergence of the laser beam was less than 0.5mrad. The root mean square (rms) value under the pump pulse energy of 250 mJ was measured

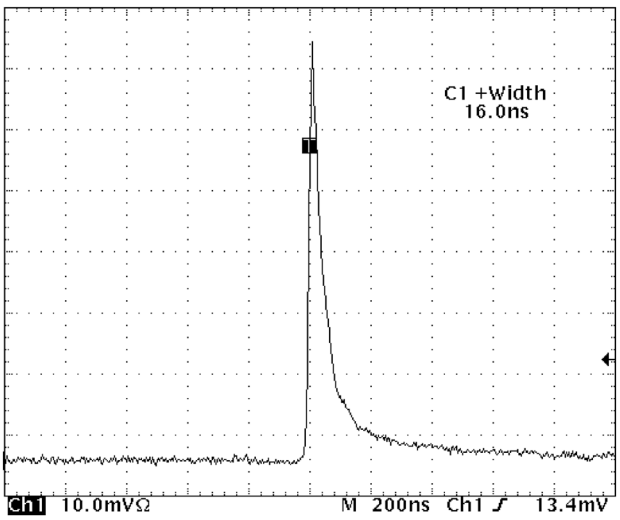

Fig. 3 Oscilloscope trace of the fundamental pulse at 1.064 μm without OPO elements

about 0.5% in 1 h. A combination of a half-wave plate (HWP) and a Brewster window (BW) was used to adjust the pump energy. A telescope device (T) was used to reshape and collimate pump beam. An aperture (D) was placed after the telescope lens to adjust the pump beam diameter. The diameters of the pump beam were 4.8 and 4.6 mm in the vertical and horizontal orientation, respectively. It is a little smaller than the crystal aperture for reducing the pump power intensity. M1 and M2 were general high reflection mirrors at 1.064 μm to adjust the pump incident direction. B was a black body to absorb the residual pump power.

The BGSe–SSRO cavity was formed by two parallel-plane dichroic mirrors coated with dielectric reflecting films. The reflectance of the input mirror (M3) made out of calcium fluoride was >95% in the range from 1.3 to 1.6 μm, and <0.5% at the pump wavelength. The output mirror (M4) had a transmission of 10% at the idler, >97% at the signal and >98% at the pump wavelength. The physical length of the cavity was 20 mm. The signal wave was totally reflected by the output coupler to provide a relatively high Q-factor in the cavity to reduce the threshold.

The pulse energies of pump and idler waves were measured by energy meter (Newport Corp. 842-PE). For the idler wave pulse energy measurement, a filter (F) consisting of a calcium fluoride plate with a dielectric selective coating and a germanium plate was placed before the energy meter to avoid the injection of pump and signal waves. The spectrum of signal wave was measured using the optical spectrum analyzer (Yokogawa AQ6375).

3 Results and analysis

The threshold for a singly resonant OPO with single pump passing can be calculated by using Brosnan and Byer's formula [23]. The peak on-axial fluence (energy/area) threshold is given by

$$J_0(\overline{\tau} = 2\tau) = \frac{2.25}{\kappa g_s {L_{\text{eff}}}^2}\tau\left(\frac{L}{2\tau c}\ln\frac{P_n}{P_0} + 2\alpha l + \ln\frac{1}{\sqrt{R}} + \ln 2\right)^2, \quad (1)$$

where

$$\kappa = \frac{2\omega_s\omega_i d_{\text{eff}}^2}{n_s n_i n_p \varepsilon_0 c^3}, \quad (2)$$

and

$$g_s = \frac{w_p^2}{w_p^2 + w_s^2}. \quad (3)$$

Here, g_s is the signal spatial mode coupling coefficient. L_{eff} is the effective parametric gain length. Ignoring the walk-off effect, the crystal length l can be used to replace the effective parametric gain length L_{eff}. τ is the $1/e^2$ intensity half width of the pump pulse. L is the optical cavity length. c is the velocity of light in vacuum, $c = 3\times10^8$ m/s. ln (P_n/P_0) is the threshold power to noise power ratio, set as 33. α is the equal averaged absorption coefficient for the resonated signal wave. l is the BGSe crystal length. $\ln(1/\sqrt{R})$ and ln2 describe the cavity output coupling loss and the SRO operation, respectively. ω_s and ω_i are the angular frequencies for the signal and idler waves. d_{eff} is the effective nonlinear coefficient of the BGSe crystal. n_s, n_i, n_p are the refractive indices at signal, idler and pump wavelengths. ε_0 is the permittivity of vacuum, $\varepsilon_0 = 8.854\times10^{-12}$ F/m. w_p and w_s, are the Gaussian mode electric field radii for pump and signal wave.

In the calculation, the exact experimental parameters were used. The value of τ was 16 ns.The equal averaged absorption α was set as 0.01 cm^{-1}. The BGSe crystal length l is 17.3 mm. The refractive indices at signal, idler and pump wavelengths n_s, n_i, n_p, can be obtained through the published Sellmeier's equation in the Ref. [19]. In addition, for the BGSe crystal, the effective nonlinear coefficient d_{eff} was calculated with the equation of $d_{\text{eff}} = d_{16}\cos^2(54.7°) + d_{23}\sin^2(54.7°)$ to be 13.8 pm/V. Based on the parameter values above, g_s was calculated as 0.6746. The calculated result for the threshold peak on-axial fluence was 0.128.8 J/cm^2 and the peak intensity of 8.05 MW/cm^2.

The input–output characteristics for BGSe–SSRO is shown in Fig. 4. The measured threshold for the cavity length of 20 mm was about 22.1 mJ, which corresponds to the peak on-axial fluence of 0.128 J/cm^2 and the peak

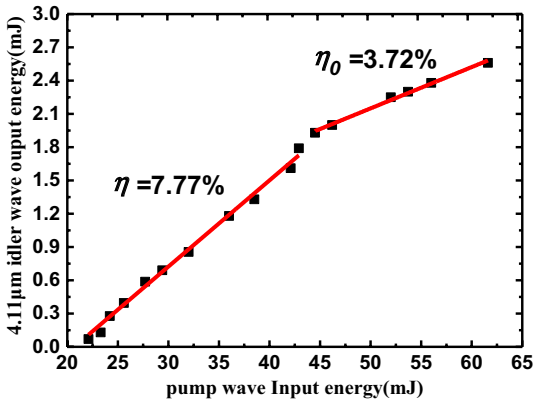

Fig. 4 Input–output characteristics of the BGSe–SSRO for a cavity length of 20 mm for the idler wavelength of 4.11 μm

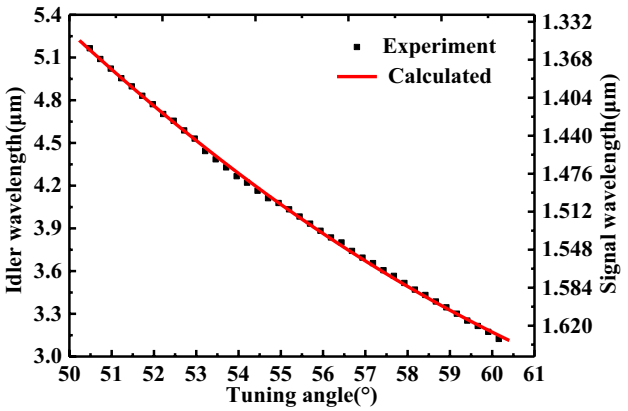

Fig. 6 Angle tuning curve of the SSRO for type I cut (θ = 54.7°) BGSe crystal

intensity of 7.97 MW/cm^2. It was in good agreement with the theoretical calculation. Under the pump energy of 61.6 mJ, the maximum idler energy at 4.11 μm amounted to 2.56 mJ, corresponding to an optical-to-optical conversion efficiency of 4.16%. However, the maximum idler wave conversion efficiency of 4.53% occurred at the pump energy of about 50 mJ. The idler wave slope efficiency was calculated from the linear fitting curves, it was 7.77% under lower pump energy level. With the increase of the pump energy, there was a saturation phenomenon for idler wave conversion with a slope efficiency of 3.72%.

Figure 5 depicts the examples of two signal wavelengths increasing with the phase matching (PM) angles, that is internal angles. By rotating the external angle of the BGSe crystal, the mid-IR spectra were recorded with an optical spectrum analyzer under the pump energy of 28.5 mJ, as shown in Fig. 6. The output laser wavelength could be tuned from 1.34 to 1.61 μm for signal wave, corresponding to the external angles from −10.38° to +13.28° or internal angles from 50.48° to 60.1° (based on the refractive index of 2.46 [20]). Because the wavelength of the idler wave was beyond the measurement range of optical spectrum analyzer, it was calculated using the law of energy conservation with the pump wavelength of 1.064 μm and the measured signal wavelength. The idler wavelength could be tuned from 3.12 to 5.16 μm. Figure 6 shows the dependence of the output wavelength on the tuning angle, it can be seen that the calculated and experimental curves coincide well.

The tunable output characteristics are shown in Fig. 7 at 28.5 mJ pump energy. It was clearly that the output energy and conversion efficiency decreased as the idler wavelength increased. The reason was that d_{eff} was decreased with the phase matching angle increasing, as shown in Fig. 7. When rotating the crystal in the large tilt angle, the energy of idler wave in 3.12–3.21 μm range had abnormal decrease, which was caused by the pump beam cutting due to limited crystal size. The idler wavelength range extended from 3.12 to 5.16 μm with a pronounced enhancement at 4.1 μm. Such phenomenon was caused by the idler wave reflection of the crystal surfaces under normal incidence, which made the SRO quasi-doubly resonant [12]. The zoomed part of the output energy curve for the tuning range of 4.2–5.1 μm has been shown in the inset of Fig. 7. It is seen that the output energies were higher than 60 μJ in this region. The lower output energy is caused by the limited crystal size. Therefore, it is deduced that the tuning range for BGSe–SSRO would be much wider with larger crystal.

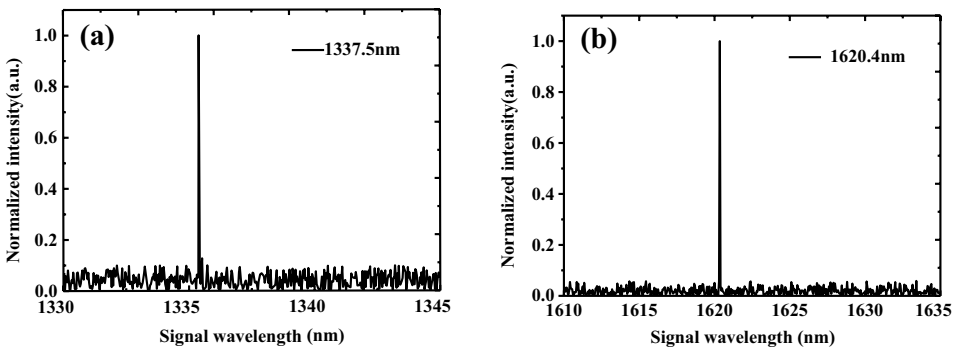

Fig. 5 Output spectra of signal wave across the OPO tuning range. **a** Signal wavelength at 1.3375 μm, **b** signal wavelength at 1.6204 μm

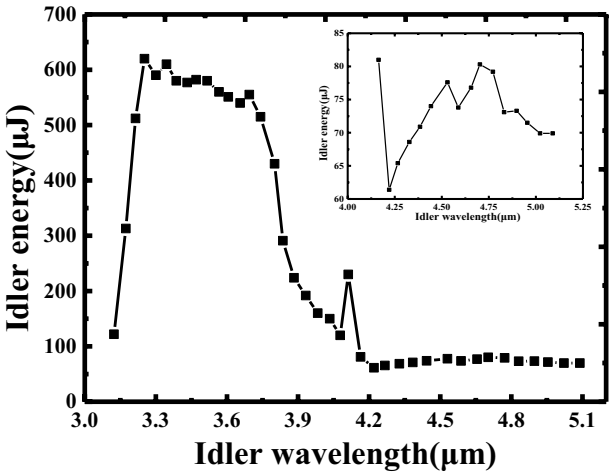

Fig. 7 Tuning output characteristics of the BGSe–SSRO at an incident pump energy of 28.5 mJ

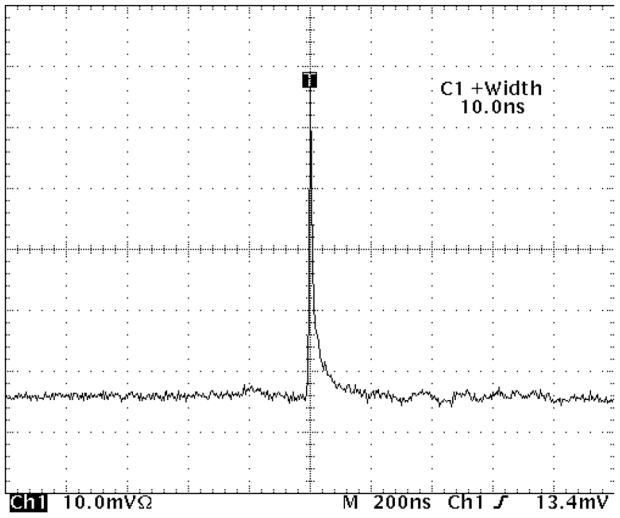

Fig. 9 Oscilloscope traces of 1.436 μm signal wave at the pump energy of 50 mJ

The distribution of the beam cross section at a wavelength of 4.11 μm was detected with an IR Pyrocam III camera (Ophir Corp.). Figure 8 presents the near- and far-field intensity distributions at the distances of 5 and 80 cm from the output window, respectively. Comparing the Fig. 8a, b, the divergence of the BGSe–SSRO beam is about 10 mrad. In addition, the FWHM pulse duration of signal wavelength was about 10 ns at the pump energy of 61.6 mJ, as shown in Fig. 9. Therefore, it could be conjectured that the pulse duration of idler wave was in the order of about 10 ns. Therefore, the peak power of idler wave amounted to about 256 kW.

4 Conclusion

In conclusion, we have demonstrated the Nd:YAG laser-pumped SSRO based on the non-oxide BGSe crystal. The tuning MIR wavelengths in the range of 1.61–1.34 and 3.12–5.16 μm were continuously obtained. The maximum pulse energy of 2.56 mJ at 4.11 μm with 10 Hz repetition rate has been obtained. The peak power of signal wave amounted to about 256 kW. Therefore, an effective high pulse energy MIR laser can be realized through BGSe–SSRO, which has great potential for the development of commercial nanosecond MIR OPOs. To the best of our knowledge, this is the highest single pulse energy for such a type BGSe–SSRO laser. It is expected that further improvement will be implemented by improving the BGSe crystal quality and cavity mirror coating. Such a high-energy MIR laser can find numerous applications in several areas, such as the military region, atmospheric pollution detection, and so on.

Acknowledgements National Basic Research Program of China (973) (2015CB755403, 2014CB339802); National key research and development projects (2016YFC0101001); National Natural Science Foundation of China (61107086, 61471257, 61275102, 51472251); Natural Science Foundation of Tianjin (14JCQNJC02200); The Science and Technology Support Program of Tianjin (13ZCZDSF02300,

Fig. 8 Idler intensity distributions at the OPO output in the near field and far-field

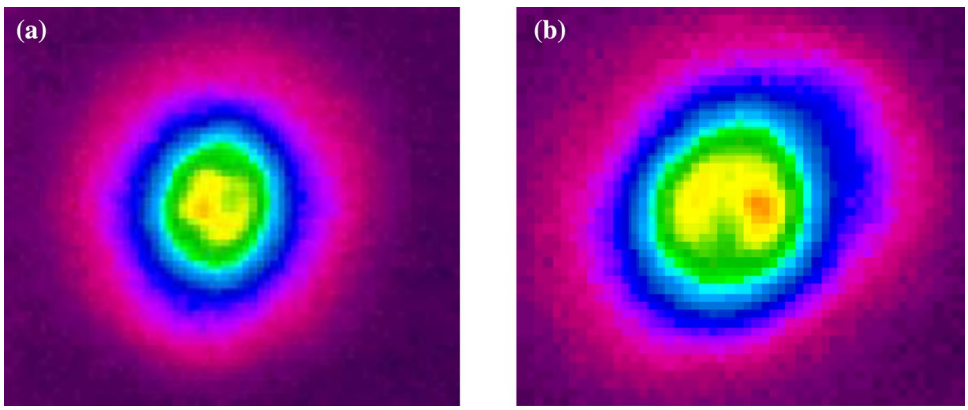

14ZCZDGX00030); Postdoctoral Science Foundation of Chongqing (Xm2016021).

References

1. V. Petrov, Frequency down-conversion of solid-state laser sources to the mid-infrared spectral range using non-oxide nonlinear crystals. Prog. Quantum Electron. **42**, 1–106 (2015)
2. J.T. Lin, J.L. Montgomery, Generation of tunable mid-ir (1.8–2.4 μm) laser from optical parametric oscillation in KTP. Opt. Commun. **75**(3–4), 315–320 (1990)
3. A.H. Kung, Narrowband mid-infrared generation using $KTiOAsO_4$. Appl. Phys. Lett. **65**(9), 1082–1084 (1994)
4. S. Sanders, R.J. Lang, L.E. Myers, M.M. Fejer, R.L. Byer, Broadly tunable mid-IR radiation source based on difference frequency mixing of high power wavelength-tunable laser diodes in bulk periodically poled $LiNbO_3$. Electron. Lett. **32**(3), 218–219 (1996)
5. E.O. Ammann, J.M. Yarborough, Optical parametric oscillation in proustite. Appl. Phys. Lett. **17**, 233–235 (1970)
6. Y.X. Fan, R.C. Eckardt, R.L. Byer, R.K. Route, R.S. Feigelson, $AgGaS_2$ infrared parametric oscillator. Appl. Phys. Lett. **45**, 313–315 (1984)
7. V. V. Badikov, A $HgGa_2S_4$ optical parametric oscillator. Quantum Electron. **33**(33), 831–832 (2003)
8. V.V. Badikov, A.K. Don, K.V. Mitin, A.M. Seryogin, V.V. Sinaiskii, N.I. Schebetova, Optical parametric oscillator on an $Hg_{1-x}\,Cd_x\,Ga_2\,S_4$ crystal. Quantum Electron. **35**, 853–856 (2005)
9. J.J. Zondy, V. Vedenyapin, A. Yelisseyev, S. Lobanov, L. Isaenko, V. Petrov, $LiInSe_2$ nanosecond optical parametric oscillator. Opt. Lett. **30**, 2460–2462 (2005)
10. V. Petrov, P.G. Schunemann, K.T. Zawilski, T.M. Pollak, Noncritical singly resonant optical parametric oscillator operation near 6.2 microm based on a $CdSiP_2$ crystal pumped at 1064 nm. Opt. Lett. **34**, 2399–2401 (2009)
11. A. Tyazhev, V. Vedenyapin, G. Marchev, L. Isaenko, D. Kolker, S. Lobanov, V. Petrov, A. Yelisseyev, M. Starikova, J.J. Zondy, Singly-resonant optical parametric oscillation based on the wide band-gap mid-IR nonlinear optical crystal $LiGaS_2$. Opt. Mater. **35**, 1612–1615 (2013)
12. A. Tyazhev, D. Kolker, G. Marchev, V. Badikov, D. Badikov, G. Shevyrdyaeva, V. Panyutin, V. Petrov, Midinfrared optical parametric oscillator based on the wide-bandgap $BaGa_4S_7$ nonlinear crystal. Opt. Lett. **37**, 4146–4148 (2012)
13. L.A. Pomeranz, P.G. Schunemann, D.J. Magarrell, J.C. McCarthy, K.T. Zawilski, D.E. Zelmon, 1-μm-pumped OPO based on orientation-patterned GaP. Proc. SPIE 9347 (2015)
14. J.Y. Yao, D.J. Mei, L. Bai, Z.S. Lin, W.L. Yin, P.Z. Fu, Y.C. Wu, $BaGa_4Se_7$: a new congruent-melting IR nonlinear optical material. Inorg. Chem. **49**(20), 9212–9216 (2010)
15. V. Badikov, D. Badikov, G. Shevyrdyaeva, Phase-matching properties of $BaGa_4S_7$ and $BaGa_4Se_7$: wide-bandgap nonlinear crystals for the mid-infrared. Phys. Status Solidi RRL **5**(1), 31–33 (2011)
16. E. Boursier, P. Segonds, J. Debray, P.L. Inácio, V. Panyutin, V. Badikov, D. Badikov, V. Petrov, B. Boulanger, Angle noncritical phase-matched second-harmonic generation in the monoclinic crystal $BaGa_4Se_7$. Opt. Lett. **40**(20), 4591–4594 (2015)
17. X. Zhang, J.Y. Yao, W.L. Yin, Y. Zhu, Y.C. Wu, C.T. Chen, Determination of the nonlinear optical coefficients of the $BaGa_4Se_7$ crystal. Opt. Express **23**(1), 552–558 (2015)
18. J.Y. Yao, W.L. Yin, K. Feng, X.X. Li, D.J. Mei, Q.M. Lu, Y.B. Nie, Z.W. Zhang, Z.G. Hu, Y.C. Wu, Growth and characterization of $BaGa_4Se_7$ crystal. J. Cryst. Growth **346**(1), 1–4 (2012)
19. F. Yang, J.Y. Yao, H.Y. Xu, K. Feng, W.L. Yin, F.Q. Li, J. Yang, S.F. Du, Q.J. Peng, J.Y. Zhang, D.F. Cui, Y.C. Wu, C.T. Chen, Z.Y. Xu, High efficiency and high peak power picosecond mid-infrared optical parametric amplifier based on BaGa4Se7 crystal. Opt. Lett. **38**(19), 3903–3905 (2013)
20. F. Yang, J.Y. Yao, H.Y. Xu, F.F. Zhang, N.X. Zhai, Z.H. Lin, N. Zong, Q.J. Peng, J.Y. Zhang, D.F. Cui, Y.C. Wu, C.T. Chen, Z.Y. Xu, Midinfrared optical parametric amplifier with 6.4–11 μm range based on $BaGa_4Se_7$. IEEE Photon. Technol. Lett. **27**(10), 1100–1103 (2015)
21. J.H. Yuan, C. Li, B.Q. Yao, J.Y. Yao, X.M. Duan, Y.Y. Li, Y.J. Shen, Y.C. Wu, Z. Cui, T.Y. Dai, High power, tunable mid-infrared $BaGa_4Se_7$ optical parametric oscillator pumped by a 2.1 μm Ho:YAG laser. Opt. Express **24**, 6 (2016)
22. N.Y. Kostyukova, A.A. Boyko, V. Badikov, D. Badikov, G. Shevyrayaeva, V. Panyutin, G.M. Marchev, D.B. Kolker, V. Petrov, Widely tunable in the mid-IR $BaGa_4Se_7$ optical parametric oscillator pumped at 1064 nm. Opt. Lett. **41**(15), 3667–3670." (2016)
23. S. Brosnan, R.L. Byer, Optical parametric oscillator threshold and linewidth studies. IEEE J. Quantum Electron. **QE-15**(6), 415–431 (1979)